

Spectral and Dynamic Properties of Excitons and Biexcitons in Type-II Semiconductor Nanocrystals

S. A. Ivanov[†] and M. Achermann^{‡,§,*}

[†]Los Alamos National Laboratory, Los Alamos, New Mexico 87545, United States, [‡]Physics Department, University of Massachusetts Amherst, Amherst, Massachusetts 01003, United States, and [§]Lucerne University of Applied Sciences and Arts, 6048 Horw, Switzerland

ABSTRACT Using time-resolved photoluminescence spectroscopy, we analyze single and multiexciton emission energies and decay dynamics of CdS/ZnSe core/shell nanocrystals (NCs). The NCs exhibit a characteristic type-II band alignment that leads to spatially separated charges; this effect is at the origin of long radiative exciton lifetimes, repulsive biexciton interaction energies, and reduced Auger recombination efficiencies. We determine these properties as a function of ZnSe shell thickness and find that the exciton emission energies and the decay times depend little on this parameter. In contrast, the spectral and dynamic properties of biexcitons vary strongly with the shell thickness. The considerable shell dependence of the biexciton decay lets us conclude that the associated Auger process involves the excitation of holes localized in the ZnSe shell. In NCs with thick shells, the large blue shift of the biexciton emission energy is mainly caused by Coulomb repulsion between electrons localized in the CdS core. The different sensitivity of exciton and multiexciton characteristics on the ZnSe shell thickness provides a unique opportunity to tune them independently.

KEYWORDS: nanocrystals · quantum dots · type-II · time-resolved spectroscopy · dynamics · biexcitons · Auger recombination

Composition-, shape- and size-tunable semiconductor nanocrystals (NCs) provide ideal systems to study charge carrier interactions in nano-scale structures with designed electron and hole wave functions. Strong quantum confinement in NCs leads to size-tunable emission and absorption properties,¹ large exciton interaction energies,^{2–4} and enhanced multiexciton processes, including ultrafast Auger recombination⁵ and Auger heating.⁶ Whereas in conventional type-I NCs electron and hole wave functions are confined within the same spatial location, it has been shown recently that the composition of core/shell NCs can be designed such that the band alignment at the core/shell interface is opposite for electrons and holes.^{7–11} Consequently, in these type-II NCs, electron and hole wave functions are spatially separated, affecting dramatically such properties as emission wavelengths,^{7–10} radiative lifetimes,^{11–15} and optical gain. The latter can occur with single excitons in type-II

NCs,^{16,17} in contrast to type-I NCs, in which optical gain requires the excitation of multiple excitons.¹⁸

In this report, we discuss the dynamic and spectral properties of excitons and biexcitons in type-II NCs, and we show how they depend on the shell thickness of the heterostructured NCs. In the single exciton regime, we demonstrate that the emission is substantially red-shifted and the radiative recombination process slowed down upon encapsulating the CdS core with a ZnSe shell and creating a spatial separation between electron and hole wave functions. Longer exciton lifetimes are desirable for photovoltaic applications, in which the charge separation process competes with exciton recombination. While the presence of the ZnSe shell modifies substantially the exciton properties, its specific thickness affects them minimally. In contrast, the spectral and dynamic properties of biexcitons that we observe at high excitation densities depend significantly on the shell thickness. The repulsive biexciton energy shift, which is at the origin of the single exciton lasing capabilities,^{16,17} is more pronounced for larger electron–hole separations in NCs with thick shells because Coulomb attraction between opposite charges is reduced and Coulomb repulsion between electrons in the core start dominating. The ZnSe shell thickness has an even more dramatic effect on the decay of biexcitons that is governed by nonradiative Auger recombination. This dependence that leads to very long Auger lifetimes up to 1 ns in NCs with thick shells lets us conclude that the Auger process involves the excitation of a hole in the ZnSe shell. Our experimental results from type-II NCs with varying shell thicknesses demonstrate the freedom to tune the spectral and

*Address correspondence to marc.achermann@hslu.ch.

Received for review June 16, 2010 and accepted September 21, 2010.

Published online September 27, 2010. 10.1021/nn101357q

© 2010 American Chemical Society

dynamic properties of biexcitons without affecting exciton properties substantially.

RESULTS AND DISCUSSION

For our studies we synthesized colloidal core/shell CdS/ZnSe nanocrystals with type-II conduction and valence band alignments at the core/shell interface that results in spatially separated excited electrons and holes (Figure 1a).¹⁹ We produced a series of 7 type-II NC samples with an identical CdS core of 1.9 nm radius (determined from the 425 nm emission peak) and with varying shell thicknesses that resulted in emission wavelengths between 537 and 561 nm (see Figure 1b). As a result of weakened quantum confinement, a thicker shell corresponds to a longer emission wavelength. We have shown previously that emission at shorter and longer wavelengths can be obtained with smaller and larger CdS core sizes, respectively.¹⁶ The large spectral shift between emission energies of the core and the core/shell NCs is a clear indication of the designed type-II band alignment. We then used time-resolved photoluminescence (PL) spectroscopy to measure exciton and biexciton energies and dynamics in these type-II NCs. The samples were excited at ~ 400 nm with femtosecond-scale laser pulses, and the emission was spectrally and temporally resolved. The employed time-correlated single photon counting system provided a time resolution of ~ 70 ps that was sufficient to study the dynamics of excitons and biexcitons in type-II NCs, as will be shown below.

Single Exciton Regime. At low excitation densities, the NC emission is characterized by its wavelength and radiative lifetime that are relevant to many applications, including light emitting and harvesting devices. As shown in Figure 1b, the emission wavelength increases with increasing ZnSe shell thickness that is primarily a result of the weakened hole confinement (Figure 1a). However, this energy shift is comparably small, since the confinement energy is rather small for holes with a large effective mass. In contrast, large wavelength tuning can be obtained by varying the CdS core size that modifies the larger confinement energy of the lighter electrons.¹⁶

To study radiative lifetimes in type-II NCs, we excited the NCs with $\sim 10 \mu\text{J}/\text{cm}^2$ pulses. Since variations in the pump fluence did not change the PL dynamics or spectra, we conclude that the applied excitation density generates predominantly single excitons in the NCs. In Figure 2a we show the PL decay dynamics of the NCs with the thinnest and thickest ZnSe shells recorded at the peak emission wavelength of each sample. A clear difference between the two is apparent, with a faster PL decay for the thin-shell NCs. The NCs have a rather high quantum yield of 30–35%, and spectrally resolved PL dynamics indicate that energy transfer due to potential NC agglomeration is negligible in most samples.²⁰ As concluded previously,²¹ the dynamics at

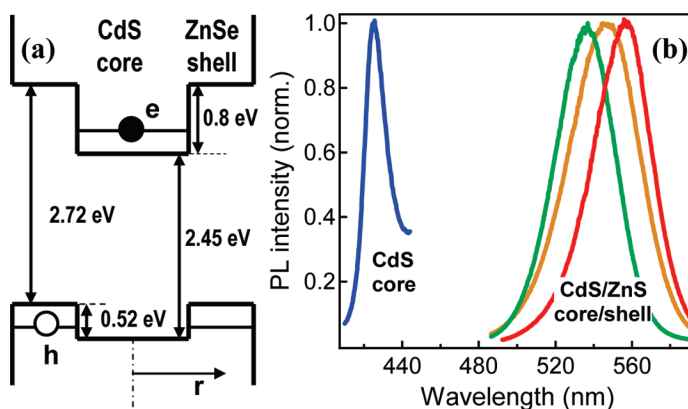


Figure 1. (a) Schematics of the conduction and valence band alignments in CdS/ZnSe type-II NCs that lead to spatially separated excited electrons and holes. (b) Emission spectra of CdS core and CdS/ZnSe core/shell NCs that have the same core but different shell thicknesses.

short time delay is dominated by NCs with nonradiative decay channels that give rise to the nonideal quantum yield, while the decay at long time delays is dominated by radiative recombination of NCs with ideal emission efficiencies. Therefore, we determine the radiative lifetime from a fit with a stretched exponential function, $PL_0 e^{-(kt)^\beta}$, to the PL decay dynamics between 10 and 100 ns. The radiative lifetime is then the first moment of this function: $\langle \tau \rangle = \Gamma(\beta^{-1})/k\beta$, where $\Gamma(x)$ is the gamma function. We chose to fit the PL dynamics with a stretched rather than a single exponential function because sample inhomogeneities cause a distribution of decay times. In Figure 2b we plot the radiative lifetimes obtained from different samples as a function of their peak emission wavelengths. NCs with the thinnest shell (shortest emission wavelength) exhibit a radiative lifetime of ~ 23 ns that is close to the 19 ns of the CdS core NCs.²² The increase in ZnSe shell thickness leads to an increase of the radiative lifetime up to ~ 45 ns.

This result can be well rationalized by considering that the radiative lifetime is inversely proportional to the overlap integral defined as $\Theta = |\langle \psi^h | \psi^e \rangle|^2$, between the electron and hole wave functions ψ^e and ψ^h , respectively.^{12–15} In type-II core/shell NCs, the electron–hole separation increases with the shell thickness,²³ and as such, the overlap integral becomes smaller and the radiative lifetime increases, which is consistent with our measurements. If we associate the radiative lifetime of the CdS core with a spatial overlap of 1, we can deduce the spatial overlap integral for the type-II NCs from the radiative lifetimes: $\Theta = \tau_{\text{CdS}}/\tau_{\text{CdS/ZnSe}}$. We determined τ_{CdS} of appreciable quantum yield (5–10%) CdS NCs by applying the same procedure as presented here,²² namely by analyzing the long time PL decay that is dominated by radiative recombination even if the NC's quantum yield is nonideal.²¹ Figure 2b indicates that the overlap integral is reduced to less than 50% but remains finite even for relatively thick shells and does not vanish as predicted

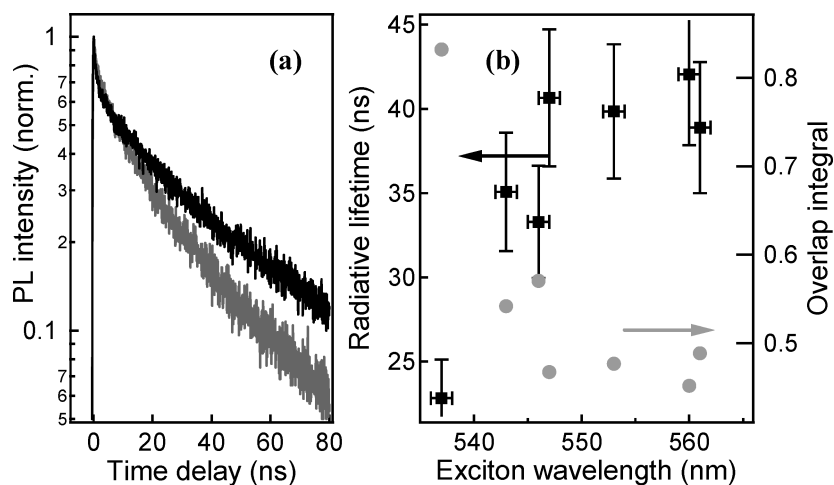


Figure 2. Single exciton regime: (a) Normalized PL decay dynamics of type-II NCs with a thin and thick (gray and black lines and emission wavelengths of 537 and 560 nm, respectively) shell. The excitation density is $\sim 10 \mu\text{J}/\text{cm}^2$. (b) Spectral overlap (gray circles) calculated from radiative lifetimes (black squares) that are obtained from PL decay dynamics as a function of exciton emission wavelength.

by theoretical calculations.²³ This can be explained by Coulomb attraction between the electron in the core and the hole in the shell that keeps the hole in the vicinity of the core even for increasingly thick shells. Such Coulomb interactions were neglected in the calculations of the electron and hole wave functions,²³ explaining the quantitative differences with our measurements. Despite the difference in absolute values, experimental and theoretical trends are in agreement qualitatively.

Biexciton Regime. In recent years, many studies have shown that multiple excitons interact much stronger in NCs than in their bulk counterparts, giving rise to such phenomena as ultrafast nonradiative Auger recombination,⁵ delayed carrier cooling,⁶ and large spectral shifts.^{2–4} Here, we are interested in the spectral and dynamic properties of biexcitons when varying the shell thickness of type-II NCs, and how these properties compare with type-I NCs. It has been shown before that biexcitons in type-I NCs display a characteristic red shift in their emission spectrum that is caused by Coulomb attraction between the excitons. The biexciton binding energy becomes larger for smaller NCs due to enhanced Coulomb interactions in smaller volumes. However, for very small NCs, the binding energy is again reduced.³ The dynamics of biexcitons in NCs is dominated by nonradiative Auger recombination. In this process an electron–hole pair recombines by exciting an additional electron or hole to a higher energy level (without emitting a photon). Auger recombination occurs in the tens of picosecond range in type-I NCs, and its rate is inversely proportional to the NC volume.⁵

To study the dynamics and interaction energies of biexcitons in type-II CdS/ZnSe NCs, we increased the pump fluence of the excitation pulse and analyzed the PL dynamics. In Figure 3a, we show the PL decays obtained with different excitation densities in the range

50–750 $\mu\text{J}/\text{cm}^2$ from type-II NCs with exciton emission wavelength of 546 nm. At high excitation densities, the time-resolved PL displays a pronounced fast decay that is negligible at low excitation levels. This accelerated decay in NC emission has previously been associated with efficient nonradiative Auger recombination of multiexcitons.³ In Figure 3b, we compare the amplitude of the fast-decaying component with the PL intensity at long time delays, $\Delta t = 5$ ns, as a function of excitation density. The latter increases linearly and then saturates, while the fast amplitude displays an initial quadratic intensity dependence followed by a slight saturation behavior. These very different intensity dependencies indicate that the PL intensity at long time delays is due to exciton recombination, while the fast initial component is caused by biexciton emission.³ From the saturation behavior of the exciton emission, we can deduce the absorption cross-section σ of the NCs. Since all multiexcitons eventually decay into single excitons, the PL at long time delays is proportional to the probability that a NC has been excited that is $1 - P_0$. P_0 is the probability that a NC is not excited and given by Poisson statistics, $P_0 = e^{-\sigma I / \hbar \omega}$, in which I and $\hbar \omega$ are the intensity and the photon energy of the excitation pulse, respectively. Hence, by fitting the intensity dependence of the exciton emission to a function proportional to $1 - P_0$, we obtain absorption cross-sections for the type-II CdS/ZnSe core/shell NCs in the range of $0.8 - 1.8 \times 10^{-15} \text{ cm}^2$ (Figure 3c). Knowing the absorption cross-section we can determine the average exciton number per NC, $\langle N \rangle = \sigma I / \hbar \omega$. For the measurements in Figure 3a, $\langle N \rangle$ varies in the range of 0.14–2.1, confirming that the intensity dependent PL traces indicate the transition between single and biexciton regime.

Characteristic for the Auger recombination process of biexcitons is their decay rate, Γ_{XX} , that we deduce from the fast decaying PL signal at high excitation den-

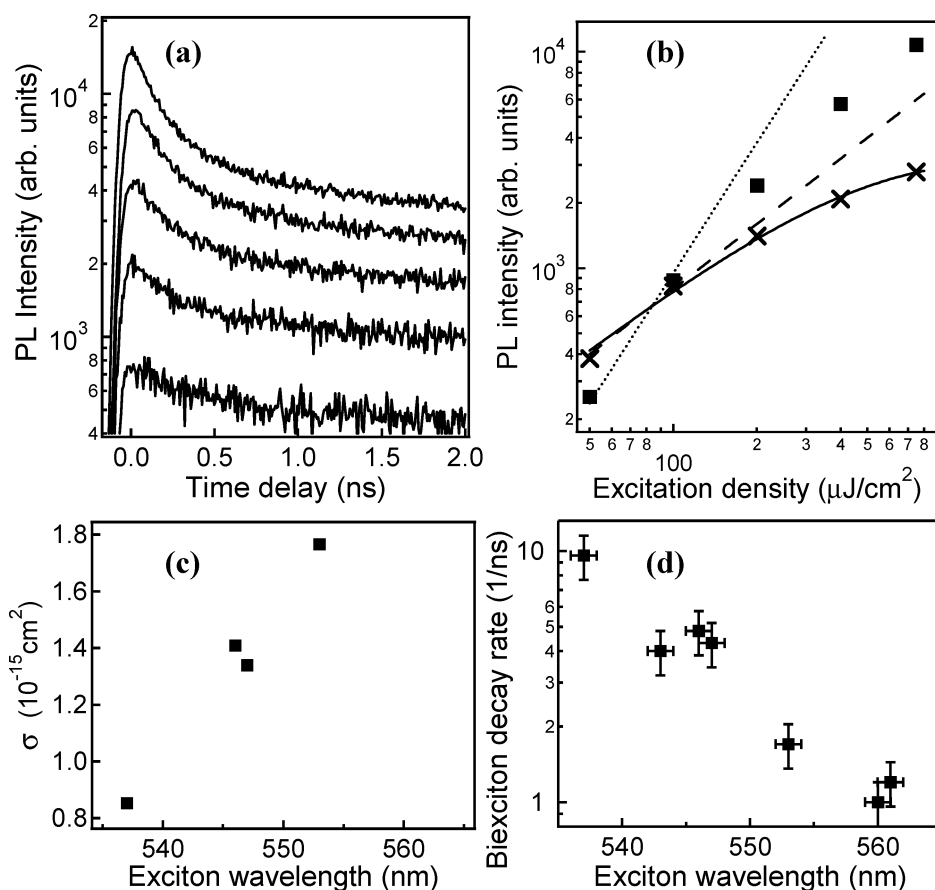


Figure 3. Dynamic properties in the multiexciton regime: (a) PL decay dynamics at varying excitation densities between 50 and 750 $\mu\text{J}/\text{cm}^2$. The excitation density is roughly doubled between each measurement. (b) Excitation density dependence of the initial fast decaying component (squares) and the PL amplitude at ~ 5 ns (crosses) fitted with the saturation function (solid line). Linear and quadratic power dependencies are indicated as dashed and dotted lines, respectively. (c) Absorption cross-sections obtained from saturation curves. (d) Biexciton decay rate as a function of exciton emission wavelength.

sities (Figure 3d). We take into account a small short-lived component caused by charge trapping that is present in PL decays even at low excitation levels. We find that Γ_{xx} decreases with increasing exciton wavelength and, thereby, with increasing shell thickness. Γ_{xx} is in the 1–10 ns⁻¹ range, significantly slower than in conventional type-I NCs.^{3,5} It is noteworthy that novel type-I NCs with softened confinement potentials have shown strongly weakened Auger processes.²⁴ The Auger recombination process can be viewed as a two step process consisting of exciton recombination and energy transfer to the remaining electron or hole.¹¹ The first process is described by the radiative decay time and slows down with increasing shell thickness, as a consequence of the reduced spatial overlap (Figure 2b). This effect is rather weak and cannot account for the total variation of Γ_{xx} . The second, energy transfer step accounts for the volume dependence of the Auger rate in type-I NCs^{3,5} and must be the major factor that leads to the strong shell thickness dependence of Γ_{xx} . Since in CdS/ZnSe NCs the shell thickness mainly affects the hole wave function, we conclude that in the Auger process, the exciton recombination energy is transferred to the hole.

The interaction between multiple excitons affects not only their lifetimes but also causes a spectral shift of their emission energy. We show here that the energy shift associated with biexciton emission in type-II NCs differs strongly from that of type-I NCs. In Figure 4a, we compare the PL spectra at high excitation density ($\langle N \rangle$

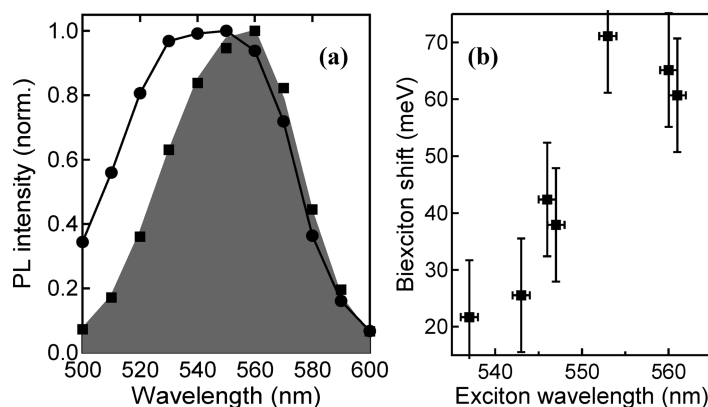


Figure 4. Spectral properties in the multiexciton regime: (a) Normalized time-resolved spectra at $\Delta t = 0$ and 2 ns (filled circles and squares, respectively) obtained with 200 $\mu\text{J}/\text{cm}^2$ excitation pulses. For comparison we show the $\Delta t = 0$ ps spectra obtained with 25 $\mu\text{J}/\text{cm}^2$ pulses (gray shaded area). (b) Biexciton energy shift Δ_{xx} as a function of exciton emission wavelength.

= 0.7) with the time delays $\Delta t = 0$ ps and 2 ns and at low excitation density ($\langle N \rangle = 0.1$) with $\Delta t = 0$ ps. Here, the zero time delay refers to the moment when the PL signal at the single exciton wavelength is fully developed after laser excitation. Within the ps scale time resolution of our setup, excitons and multiexcitons that are excited with an excess energy of ~ 0.8 eV are mostly relaxed to their ground state.²⁵ Figure 4a shows that the PL spectrum at $\Delta t = 2$ ns obtained at high excitation density overlaps with the low excitation density PL spectrum and, therefore, can be assigned to single exciton emission. In contrast, the high excitation density PL spectrum at $\Delta t = 0$ ps is broadened toward shorter wavelengths. Applying Poisson statistics with an average exciton number ($\langle N \rangle = 0.7$), we determine the percentage of NCs with no excitation, single excitons, biexcitons, and higher multiexcitons to be 50, 35, 12, and 3%, respectively. Hence, the PL spectra at $\Delta t = 0$ ps must originate primarily from excitons and biexcitons. The biexciton emission at short wavelengths decays quickly, as we have seen above, resulting in single exciton emission at long time delays. Such spectral properties are consistent with time-resolved emission measurements of type-I NCs.³ The main and distinct difference is that in type-II NCs the biexciton emission is blue-shifted toward higher photon energies, while in type-I NCs the biexcitonic emission is red-shifted with respect to the single exciton emission. The appearance of biexciton emission at shorter wavelengths than the single exciton emission is crucial for enabling optical gain in type-II NCs with single excitons.¹⁶

In order to quantify the energy shift between excitons and biexcitons, we need to separate the two contributions in the $\Delta t = 0$ ps PL spectra obtained at high excitation densities. Biexciton spectra can be obtained by subtracting the single exciton emission contribution with a procedure described in ref 3 that takes into account the single exciton decay dynamics and the Poisson distribution of excitons and biexcitons in NCs. Applying such a procedure, the biexciton energy shift Δ_{xx} is given by the difference in energy between the biexciton and single exciton emission spectra. In Figure 4b, Δ_{xx} is shown as a function of exciton emission wavelength and, as such, of ZnSe shell thickness. Because of the spatially separated electrons and holes, Δ_{xx} is positive and indicates Coulomb repulsion¹⁶ in contrast to the negative biexciton energy shift in type-I NCs that is caused by attractive interactions. The Δ_{xx} increases up to ~ 70 meV with increasing shell thickness, because the electron–hole separation increases, and therefore, attractive interactions between electrons and holes diminish and the positive interaction energy caused by Coulomb repulsion of the two core electrons becomes dominant. These results are consistent with theoretical modeling based on first-order perturbation calculations.²³ It is worth noting that the biexciton energy shifts are significantly larger in CdS/ZnSe than in CdTe/

CdSe NCs for similar dimensions.¹¹ CdTe/CdSe NCs also exhibit a type-II band alignment, but holes are localized in the core and electrons in the shell. Since holes are less confined than electrons, Coulomb repulsion is weaker in CdTe/CdSe NCs than in the CdS/ZnSe NCs studied here.

For a simple, order of magnitude estimate of Δ_{xx} , we consider the limiting case of a very thick shell, such that the electron–hole and the hole–hole interactions are negligible, and Δ_{xx} is dominated by the electron–electron interaction, $W^{ee} \propto (\epsilon r)^{-1}$, in which r is the electron–electron separation, and ϵ is the high-frequency dielectric constant. Taking the radius of the CdS core (1.9 nm) as an average value for the electron–electron separation and using 5.3 for the high-frequency dielectric constant of CdS, we obtain $W^{ee} = 143$ meV. It is noteworthy that such a simplified theoretical approach that is based solely on electrostatics of point charges provides the right order of magnitude for the measured Δ_{xx} in type-II NCs with thick ZnSe shells. The difference between W^{ee} and Δ_{xx} arises from the neglected core–shell interface polarization and the attractive electron–hole Coulomb interactions that both reduce the biexciton energy shift.²³

CONCLUSIONS

In this report we discussed the dynamic and spectral properties of excitons and biexcitons in type-II CdS/ZnSe core/shell nanocrystals (NCs) with varying shell thicknesses. We demonstrated that the biexcitons are strongly affected by the shell thickness, while the single exciton properties vary little. In the single exciton regime, we showed that, with increase in the shell thickness, the exciton emission red-shifts by 30 nm and that the radiative lifetime and the spatial overlap between electron and hole wave functions decrease by a factor of 1.75. At higher excitation densities, short-lived biexciton emission was observed and determined to be spectrally blue-shifted with respect to the single exciton emission from the same system. Such a positive biexciton energy shift can be well rationalized by Coulomb repulsion between like charges in the core and the shell components of the type-II NCs. The lifetimes of biexcitons are longer in type-II than in type-I NCs and amount to several hundreds of picoseconds, limited by nonradiative Auger recombination. Our measurements with CdS/ZnSe NCs indicate that the Auger process involves the excitation of a hole in the ZnSe shell. Within the studied range of shell thicknesses, the biexciton energy shift and the Auger recombination rate vary significantly more than the exciton properties. Therefore, the shell thickness is an ideal parameter to tune biexciton properties almost independently from the single exciton characteristics, which is important for the use of these type-II NCs in potential applications that include solar cell or optical gain materials.

EXPERIMENTAL DETAILS

CdS/ZnSe Nanocrystals Synthesis. We synthesized colloidal core/shell CdS/ZnSe nanocrystals following previously published procedure.²⁶ The growth of the CdS core was conducted according to the modified procedure by Cao *et al.*,²⁷ in which a mixture of Cd(AcO)₂ · 2H₂O, myristic acid, and a 0.1 M sulfur solution in 1-octadecene (ODE) was heated to 240 °C until the desired size of CdS cores was achieved. After the core growth, special attention was devoted to remove any possible adsorbed byproduct from the surface *via* several, 30 min-long ultrasonic treatments of CdS cores in the presence of TOPO or pyridine excess. To overcoat the CdS cores with ZnSe shells, 0.45 M Zn(AcO)₂ solution in tri-*n*-octylphosphine (TOP) and 1 M Se solution in TOP were mixed together in pure TOP and added dropwise to the CdS NC solution in an ODE/octadecylamine mixture at 220 °C. After the deposition, the solution temperature was decreased to 120 °C, and the NCs were annealed at that temperature for 8–10 h. In the end, the CdS/ZnSe NCs were once precipitated with acetone and redissolved in hexane. In the synthesis of these NCs, the thorough purification of CdS cores and the relatively low ZnSe overcoating temperatures were utilized to avoid alloying between the CdS core and the ZnSe shell and to preserve a step-like alignment of electron and hole bands between core and shell materials (Figure 1a). The final shape of the core/shell product was not perfectly spherical but somewhat tetrahedral. All measurements in this report were performed with dilute NC solutions in 1 mm thick cuvettes (<10% absorption at the excitation wavelength to avoid large excitation density variations within the excited volume of NC solution).

Optical Experiments. For time-resolved PL measurements, the samples were excited at ~400 nm with femtosecond-scale laser pulses from the frequency-doubled output of a Ti:sapphire amplifier operating at a 250 kHz repetition rate. The power of the excitation beam was varied with neutral density filters to access different excitation density regimes. The NC PL was spectrally dispersed in a monochromator, detected with a single photon counting avalanche photodiode, and temporally resolved with a time-correlated single photon counting system. Time-resolved spectra were reconstructed from time-resolved PL decay measurements that were recorded at different wavelengths.

Acknowledgment. We would like to thank V.I. Klimov for stimulating discussions. This work was performed, in part, at the Center for Integrated Nanotechnologies, a United States Department of Energy, Office of Basic Energy Sciences user facility at Los Alamos National Laboratory (contract DE-AC52-06NA25396) and Sandia National Laboratories (contract DE-AC04-94AL85000).

REFERENCES AND NOTES

- Alivisatos, A. P. Semiconductor Clusters, Nanocrystals, and Quantum Dots. *Science* **1996**, *271*, 933–937.
- Kang, K. I.; Kepner, A. D.; Gaponenko, S. V.; Koch, S. W.; Hu, Y. Z.; Peyghambarian, N. Confinement-Enhanced Biexciton Binding-Energy in Semiconductor Quantum Dots. *Phys. Rev. B: Condens. Matter Mater. Phys.* **1993**, *48*, 15449–15452.
- Achermann, M.; Hollingsworth, J. A.; Klimov, V. I. Multiexcitons Confined within a Subexcitonic Volume: Spectroscopic and Dynamical Signatures of Neutral and Charged Biexcitons in Ultrasmall Semiconductor Nanocrystals. *Phys. Rev. B: Condens. Matter Mater. Phys.* **2003**, *68*, 245302.
- Caruge, J. M.; Chan, Y. T.; Sundar, V.; Eisler, H. J.; Bawendi, M. G. Transient Photoluminescence and Simultaneous Amplified Spontaneous Emission from Multiexciton States in Cdse Quantum Dots. *Phys. Rev. B: Condens. Matter Mater. Phys.* **2004**, *70*, 085316.
- Klimov, V. I.; Mikhailovsky, A. A.; McBranch, D. W.; Leatherdale, C. A.; Bawendi, M. G. Quantization of Multiparticle Auger Rates in Semiconductor Quantum Dots. *Science* **2000**, *287*, 1011–1013.
- Achermann, M.; Bartko, A. P.; Hollingsworth, J. A.; Klimov, V. I. The Effect of Auger Heating on Intraband Carrier Relaxation in Semiconductor Quantum Rods. *Nat. Phys.* **2006**, *2*, 557–561.
- Kim, S.; Fisher, B.; Eisler, H. J.; Bawendi, M. Type-II Quantum Dots: Cdte/Cdse(Core/Shell) and Cdse/ZnTe(Core/Shell) Heterostructures. *J. Am. Chem. Soc.* **2003**, *125*, 11466–11467.
- Schops, O.; Le Thomas, N.; Woggon, U.; Artemyev, M. V. Recombination Dynamics of Cdte/Cds Core-Shell Nanocrystals. *J. Phys. Chem. B* **2006**, *110*, 2074–2079.
- Yu, K.; Zaman, B.; Romanova, S.; Wang, D. S.; Ripmeester, J. A. Sequential Synthesis of Type II Colloidal Cdte/Cdse Core-Shell Nanocrystals. *Small* **2005**, *1*, 332–338.
- Xie, R. G.; Zhong, X. H.; Basche, T. Synthesis, Characterization, and Spectroscopy of Type-II Core/Shell Semiconductor Nanocrystals with ZnTe Cores. *Adv. Mater.* **2005**, *17*, 2741–2745.
- Oron, D.; Kazes, M.; Banin, U. Multiexcitons in Type-II Colloidal Semiconductor Quantum Dots. *Phys. Rev. B: Condens. Matter Mater. Phys.* **2007**, *75*, 035330.
- Balet, L. P.; Ivanov, S. A.; Piryatinski, A.; Achermann, M.; Klimov, V. I. Inverted Core/Shell Nanocrystals Continuously Tunable between Type-I and Type-II Localization Regimes. *Nano Lett.* **2004**, *4*, 1485–1488.
- Kumar, S.; Jones, M.; Lo, S. S.; Scholes, G. D. Nanorod Heterostructures Showing Photoinduced Charge Separation. *Small* **2007**, *3*, 1633–1639.
- Dorfs, D.; Franzl, T.; Osovsky, R.; Brumer, M.; Lifshitz, E.; Klar, T. A.; Eychmueller, A. Type-I and Type-II Nanoscale Heterostructures Based on Cdte Nanocrystals: A Comparative Study. *Small* **2008**, *4*, 1148–1152.
- Wang, C. H.; Chen, T. T.; Chen, Y. F.; Ho, M. L.; Lai, C. W.; Chou, P. T. Recombination Dynamics in Cdte/Cdse Type-II Quantum Dots. *Nanotechnology* **2008**, *19*, 115702.
- Klimov, V. I.; Ivanov, S. A.; Nanda, J.; Achermann, M.; Bezel, I.; McGuire, J. A.; Piryatinski, A. Single-Exciton Optical Gain in Semiconductor Nanocrystals. *Nature* **2007**, *447*, 441–446.
- Nanda, J.; Ivanov, S. A.; Achermann, M.; Bezel, I.; Piryatinski, A.; Klimov, V. I. Light Amplification in the Single-Exciton Regime Using Exciton-Exciton Repulsion in Type-II Nanocrystal Quantum Dots. *J. Phys. Chem. C* **2007**, *111*, 15382–15390.
- Klimov, V. I.; Mikhailovsky, A. A.; Xu, S.; Malko, A.; Hollingsworth, J. A.; Leatherdale, C. A.; Eisler, H. J.; Bawendi, M. G. Optical Gain and Stimulated Emission in Nanocrystal Quantum Dots. *Science* **2000**, *290*, 314–317.
- Steiner, D.; Dorfs, D.; Banin, U.; Della Sala, F.; Manna, L.; Millo, O. Determination of Band Offsets in Heterostructured Colloidal Nanorods Using Scanning Tunneling Spectroscopy. *Nano Lett.* **2008**, *8*, 2954–2958.
- Achermann, M.; Petruska, M. A.; Crooker, S. A.; Klimov, V. I. Picosecond Energy Transfer in Quantum Dot Langmuir-Blodgett Nanoassemblies. *J. Phys. Chem. B* **2003**, *107*, 13782–13787.
- Crooker, S. A.; Barrick, T.; Hollingsworth, J. A.; Klimov, V. I. Multiple Temperature Regimes of Radiative Decay in Cdse Nanocrystal Quantum Dots: Intrinsic Limits to the Dark-Exciton Lifetime. *Appl. Phys. Lett.* **2003**, *82*, 2793–2795.
- Yang, B.; Schneeloch, J. E.; Pan, Z.; Furis, M.; Achermann, M. Radiative Lifetimes and Orbital Symmetry of Electronic Energy Levels of Cds Nanocrystals: Size Dependence. *Phys. Rev. B: Condens. Matter Mater. Phys.* **2010**, *81*, 073401.
- Piryatinski, A.; Ivanov, S. A.; Tretiak, S.; Klimov, V. I. Effect of Quantum and Dielectric Confinement on the Exciton-Exciton Interaction Energy in Type II Core/Shell Semiconductor Nanocrystals. *Nano Lett.* **2007**, *7*, 108–115.
- Wang, X. Y.; Ren, X. F.; Kahen, K.; Hahn, M. A.; Rajeswaran, M.; Maccagnano-Zacher, S.; Silcox, J.; Cragg, G. E.; Efros, A. L.; Krauss, T. D. Non-Blinking Semiconductor Nanocrystals. *Nature* **2009**, *459*, 686–689.
- Peng, P.; Milliron, D. J.; Hughes, S. M.; Johnson, J. C.; Alivisatos, A. P.; Saykally, R. J. Femtosecond Spectroscopy of Carrier Relaxation Dynamics in Type II Cdte/Cdse

- Tetrapod Heteronanostructures. *Nano Lett.* **2005**, *5*, 1809–1813.
26. Ivanov, S. A.; Piryatinski, A.; Nanda, J.; Tretiak, S.; Zavadil, K. R.; Wallace, W. O.; Werder, D.; Klimov, V. I. Type-II Core/Shell CdS/ZnSe Nanocrystals: Synthesis, Electronic Structures, and Spectroscopic Properties. *J. Am. Chem. Soc.* **2007**, *129*, 11708–11719.
27. Cao, Y. C.; Wang, J. H. One-Pot Synthesis of High-Quality Zinc-Blende CdS Nanocrystals. *J. Am. Chem. Soc.* **2004**, *126*, 14336–14337.